The Journal of Chemical Physics

Coherent control of collision processes: Penning versus associative ionization

Cite as: J. Chem. Phys. **125**, 094315 (2006); https://doi.org/10.1063/1.2336430
Submitted: 22 May 2006 • Accepted: 19 July 2006 • Published Online: 06 September 2006

Carlos A. Arango, Moshe Shapiro and Paul Brumer

View Online

Export Citation

ARTICLES YOU MAY BE INTERESTED IN

Theory of Penning Ionization. I. Atoms
The Journal of Chemical Physics **52**, 3563 (1970); https://doi.org/10.1063/1.1673523

Dynamics of gas phase Ne^* + NH_3 and Ne^* + ND_3 Penning ionisation at low temperatures
The Journal of Chemical Physics **140**, 244302 (2014); https://doi.org/10.1063/1.4883517

Perspective: Ultracold molecules and the dawn of cold controlled chemistry
The Journal of Chemical Physics **145**, 150901 (2016); https://doi.org/10.1063/1.4964096

Challenge us.
What are your needs for periodic signal detection?
Watch
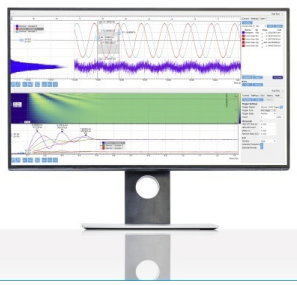
Zurich Instruments

AIP Publishing

© 2006 American Institute of Physics.

Coherent control of collision processes: Penning versus associative ionization

Carlos A. Arango
Chemical Physics Theory Group, Department of Chemistry, University of Toronto, Toronto M5S3H6, Canada and Center for Quantum Information and Quantum Control, University of Toronto, Toronto M5S3H6, Canada

Moshe Shapiro
Department of Chemistry, University of British Columbia, Vancouver V6T1Z1, Canada and Department of Chemical Physics, The Weizmann Institute, Rehovot 76100, Israel

Paul Brumer[a)]
Chemical Physics Theory Group, Department of Chemistry, University of Toronto, Toronto M5S3H6, Canada and Center for Quantum Information and Quantum Control, University of Toronto, Toronto M5S3H6, Canada

(Received 22 May 2006; accepted 19 July 2006; published online 6 September 2006)

Coherent control theory is applied to the control of $Ne^*(3s,{}^3P_2)+Ar({}^1S_0)$ collisions and computations are shown that display extensive control over these processes. Indeed we demonstrate that it is possible to essentially turn on and off the cross sections for both the Penning and associative ionization processes. This facility arises from the interference between matter waves induced by creating a linear superposition of the degenerate $M=\{-2,-1,0,1,2\}$ Zeeman sublevels of the $Ne^*(3s,{}^3P_2)$ target atom. The computations, conducted at collision energies in the 1–8 kcal/mole range, are based on combining, within the "rotating atom approximation," empirically derived and *ab initio* ionization widths. © *2006 American Institute of Physics*. [DOI: 10.1063/1.2336430]

I. INTRODUCTION

One of the major, yet unrealized, aims of coherent control[1] is the experimental demonstration of the coherent control of reactive collision events. Such control is achieved by superposing two or more scattering eigenfunctions that can interfere. Control over the interference term results in control over the scattering cross sections (for details see Ref. 1). However, required bimolecular kinematic conditions[2] make it more difficult to apply the techniques that proved successful in experimental studies of photodissociation and other unimolecular processes to bimolecular reactions. Below we theoretically demonstrate that these difficulties do not arise when one can prepare superpositions of degenerate internal states of one of the collision partners. Such is the case in collisions leading to the Penning ionization (PI) and associative ionization[3] (AI) where superpositions of the internal states of the electronically excited partner can be used. Here we computationally demonstrate extensive control over these processes, a study which we hope will motivate future experimental work.

Consider therefore controlling the collision between a metastable atom (or molecule) A^* with a ground state target atom or molecule B. The collision can lead to events in which one channel is PI, which is the ionization of the target atom and the deexcitation of the metastable species, and the other channel is AI, in which the colliding partners form an ionic dimer while emitting an energetic electron. The atoms can also remain neutral and simply scatter elastically (or inelastically) from one another.

The two ionization processes can be summarized as

$$AB^+ + e^- \leftarrow A^* + B \rightarrow A + B^+ + e^-. \quad (1)$$

These processes can only occur when $E_*(A)$, the excitation energy of the metastable species, exceeds IE(B), the energy necessary to ionize the target. For noble gases,[3] IE(B) ranges between 2 and 5 eV while $E_*(A)$ ranges between 8 and 20 eV. This fact, and the long lifetimes of some of the excited electronic states of noble gases, coupled with their relatively simple electronic structures, makes noble gases especially amenable to the experimental and theoretical study of PI and AI.

Our interest is in demonstrating that control of PI and AI total cross sections in the metastable $Ne^*(3s,{}^3P_2)$ collision with ground state $Ar({}^1S_0)$ is feasible, by preparing initial superpositions of the M states of the Ne^*, where M is the projection of the electronic angular momentum on the laboratory z axis. This control is possible since the atom-atom interaction potential depends upon M. As such, the situation is distinctly different from our previous efforts[2] to superpose states with different z-axis projections M_z of the diatomic angular momentum in atom-diatom collisions. In that case, because the interaction potential is independent of M_z, control over the differential cross section is possible, but control over the total cross section is not.

A wealth of information is available for the Ne^*+Ar sys-

a)Electronic mail: pbrumer@tikva.chem.utoronto.ca

 © 2006 American Institute of Physics

tem. In the entrance channel, optical potentials $V_{\rm opt}(r) = V_*(r) - \frac{1}{2}i\Gamma(r)$, that reproduce fairly well the total ionization cross section $\sigma^{\rm I}$, have been constructed.[4–7] For the exit channels, empirical ion-atom potentials, due to Hausamann and Morgner[8] are also available. Indeed, these parameters were even successful[9,10] in explaining the observed nonstatistical fine-structure product branching ratios.[11]

Molecular beam experiments using $Ne^*(3s,{}^3P_2)$ irradiated prior to the collision with Ar with linear or circularly polarized light show only weak polarization dependence, unlike the case of $Ne^*(3p,{}^3D_3)$.[12–14] Further, calculations of Ruf and co-workers[12,13] show that the real part of the optical potential for $Ne^*(3s,{}^3P_2)$ barely changes for the different Ω states, with $\Omega \equiv |\lambda|$, the absolute value of the projection of the electronic angular momentum on the interatomic axis, suggesting that this may not be a suitable candidate for control. However, the imaginary part of the optical potential is sensitive to Ω: Autoionization widths obtained by Drießen *et al.*[15] and Op de Beek *et al.*,[16] using *ab initio* electronic structure calculations, show that Γ varies with Ω, thereby allowing for the possibility of coherent control of the ionization cross sections.

Our results below clearly show that this is indeed an excellent system for the experimental demonstration of the coherent control of bimolecular processes. In addition to large changes in the cross sections possible via coherent control, laboratory techniques developed to deal with the Penning ionization are well suited to demonstrate control in these systems.

This paper is organized as follows: Section II introduces the theory, with the aim of establishing our notation and obtaining the basic formulas for the coherent control of the cross sections. Related material is provided in the Appendix. Section III then describes our main control results, with final conclusions provided in Sec. IV.

II. THEORY

A. The initial superposition state

The initial state of the colliding pair is given as

$$|\psi\rangle = |\psi_{\rm Ar}\rangle|\psi_{\rm Ne^*}\rangle, \tag{2}$$

where $|\psi_{\rm Ar}\rangle$ and $|\psi_{\rm Ne^*}\rangle$, the states of $Ar({}^1S_0)$ and $Ne^*(3s,{}^3P_2)$ prior to the collision, are given in a space-fixed coordinate frame as

$$|\psi_{\rm Ar}\rangle = |\phi_{\rm Ar}\rangle \exp(i\mathbf{k}^{\rm Ar}\cdot\mathbf{r}^{\rm Ar}), \tag{3a}$$

$$|\psi_{\rm Ne^*}\rangle = \sum_M |\phi^M_{\rm Ne^*}\rangle a_M \exp(i\mathbf{k}^{\rm Ne}\cdot\mathbf{r}^{\rm Ne}). \tag{3b}$$

The space-fixed (SF) vectors $\mathbf{r}^{\rm Ar}$ and $\mathbf{k}^{\rm Ar}$ ($\mathbf{r}^{\rm Ne}$ and $\mathbf{k}^{\rm Ne}$) describe the position and momentum of the Ar (Ne^*) atom. $|\phi_{\rm Ar}\rangle$ and $|\phi^M_{\rm Ne^*}\rangle$ represent the electronic states of the atoms, with $M=\{-2,-1,0,1,2\}$ designating the projection of the electronic angular momentum on the space-fixed quantization axis.

The dynamical equations are simplified by transforming them to the center of mass (c.m.)/molecular-fixed (BF) frame given as

$$\mathbf{R}_{\rm c.m.} \equiv \frac{m_{\rm Ne}\mathbf{r}^{\rm Ne} + m_{\rm Ar}\mathbf{r}^{\rm Ar}}{m_{\rm NeAr}}, \quad \mathbf{r} \equiv \mathbf{r}^{\rm Ne} - \mathbf{r}^{\rm Ar}. \tag{4}$$

In the above, $m_{\rm NeAr} \equiv m_{\rm Ne} + m_{\rm Ar}$, $\mathbf{R}_{\rm c.m.}$ is the c.m. coordinate, and $\mathbf{r}$ is the internuclear separation vector. The BF momenta are given as

$$\mathbf{K} \equiv \mathbf{k}^{\rm Ne} + \mathbf{k}^{\rm Ar}, \quad \mathbf{k} \equiv \frac{1}{m_{\rm NeAr}}[m_{\rm Ar}\mathbf{k}^{\rm Ne} - m_{\rm Ne}\mathbf{k}^{\rm Ar}]. \tag{5}$$

Substituting the above transformation in Eq. (2) results in the following expression for the initial state:

$$|\psi\rangle = e^{i\mathbf{K}\cdot\mathbf{R}_{\rm c.m.}+i\mathbf{k}\cdot\mathbf{r}}|\phi_{\rm Ar}\rangle\sum_M a_M|\phi^M_{\rm Ne^*}\rangle, \tag{6}$$

where $|\phi^M_{\rm Ne^*}\rangle$ are the Ne^* electronic wave functions. Note that $|\psi\rangle$ comprises an initial superposition state of the degenerate M eigenstates of Ne^*. As such, interference between states is possible.[2]

Because the electrons tend to follow the nuclei, the ionization widths for the colliding system $Ar({}^1S_0) + Ne^*(3s,{}^3P_2)$ mainly depend on λ, the (BF) projection of the electronic angular momentum on $\mathbf{r}$, the interatomic axis. It is therefore necessary to express the $|\phi^M_{\rm Ne^*}\rangle$ states in terms of the $|\phi^\lambda_{\rm Ne^*}\rangle$ BF states.

In this paper we adopt the "rotating atom approximation" (RAA),[17] according to which the axis of quantization of the electrons faithfully follows the internuclear separation vector. This means that the linear combination of Eq. (6) in M simply becomes a linear combination with the same coefficients in λ as the atoms approach one another. (In contrast, in the "fixed atom" approximation the electrons of the Ne^* atom remain effectively quantized along the SF Z axis during the course of the collision).

The (even parity) linear combination in the BF frame is written as

$$|\psi\rangle = |\phi_{\rm Ar}\rangle e^{i\mathbf{K}\cdot\mathbf{R}_{\rm c.m.}+i\mathbf{k}\cdot\mathbf{r}}\sum_{\Omega=0}^{2}|\phi^\Omega_{\rm Ne^*}\rangle a_\Omega, \tag{7}$$

where $\Omega \equiv |\lambda|$ and (due to the assumed even parity) $a_\Omega \equiv (a_M + a_{-M})$.

B. Scattering amplitude

The basic formulas for the scattering amplitude have been obtained in the Appendix. In this section we show how to modify those formulas and how to adapt them in the different approximations used. We write only the formulas for crossed beam experiments with the quantization axis along the internuclear momentum direction, $\hat{k}=(0,0)$.

In the RAA the scattering amplitude is related in a straightforward manner to Eqs. (A15) and (A16). Replacing the $\phi_N(\mathbf{R};\mathbf{r})$ of Eq. (A5) by the sum in Eq. (7) gives

$$V_{\varepsilon,\hat{\mathbf{k}}_\varepsilon}(\mathbf{r}) = \sum_\Omega \langle \phi_{\varepsilon,\hat{\mathbf{k}}_\varepsilon}\phi_{N-1}|H|\phi^\Omega_N\rangle_{\mathbf{R}} a_\Omega, \tag{8}$$

where $\langle\phi|H|\phi'\rangle_{\mathbf{R}}$ designates integration over the electronic coordinates $\mathbf{R}$ for all N electrons.

Following the Appendix, we find that the scattering amplitude can be written as

$$f_a(\hat{k}_f,\varepsilon,\hat{\mathbf{k}}_\varepsilon,k)=\sum_\Omega a_\Omega f_\Omega(\hat{k}_f,\varepsilon,\hat{\mathbf{k}}_\varepsilon,k), \tag{9}$$

with

$$f_\Omega(\hat{\mathbf{k}}_f,\varepsilon,\hat{\mathbf{k}}_\varepsilon,k)=\frac{\pi^{1/2}}{ik}\sum_{\ell\mu}\sum_{l}\sum_{l'} i^{l-l'}(2l+1) \times(2l'+1)^{1/2}S^{l\Omega}_{l'\ell}(\varepsilon)Y_{\ell'-\mu}(\hat{\mathbf{k}}_f)Y_{\ell\mu}(\hat{\mathbf{k}}_\varepsilon) \times\begin{pmatrix} l' & \ell & l \\ 0 & 0 & 0\end{pmatrix}\begin{pmatrix} l' & \ell & l \\ -\mu & \mu & 0\end{pmatrix}, \tag{10}$$

and $S^{l\Omega}_{l'\ell}(\varepsilon)$ defined as

$$S^{l\Omega}_{l'\ell}(\varepsilon)=-2i\frac{2\mathbf{m}\rho_\varepsilon^{1/2}}{\hbar^2}e^{i(\delta^l+\delta^{l'}_f)}\langle\psi^{l'}_\varepsilon|V^\Omega_{\varepsilon\ell}|\psi^l_d\rangle, \tag{11}$$

where $\mathbf{m}$ is the Ar–Ne reduced mass and the integration is performed over the internuclear separation $\mathbf{r}$,

$$V^\Omega_{\varepsilon\ell}=i^{-\ell}e^{-i\sigma^\ell}\langle\chi^\ell_\varepsilon Y_{\ell0}\phi_{N-1}|H|\phi^\Omega_N\rangle_{\mathbf{R}}. \tag{12}$$

Because ϕ_N and ϕ_{N-1} depend parametrically the internuclear separation $\mathbf{r}$, $V^\Omega_{\varepsilon\ell}$ is also a function of the internuclear separation.

A fair simplification is to consider $\ell=0$, i.e., only s waves of the product electron. This approximation is supported by our numerical results in the RAA using the Hickman and Morgner model[3,18,19] with α_ℓ coefficients given by Khan *et al.*[20]

C. The Ω-dependent cross sections

The Ω-dependent partial wave S matrix, $S^{l,\Omega}_{l'\ell}(\varepsilon)$ is related in the Hickman and Morgner model[3,18,19] to the ionization width $\Gamma_\Omega(r)$ through the relations

$$S^{l,\Omega}_{l'\ell}(\varepsilon)=-2i\frac{2\mathbf{m}\rho_\varepsilon^{1/2}}{\hbar^2}e^{i(\delta^l+\delta^{l'}_f)}\langle\psi^{l'}_\varepsilon|V^\Omega_{\varepsilon\ell}|\psi^l_d\rangle, \tag{13}$$

for PI, and

$$S^{l,\Omega}_{l'\ell}(\varepsilon)=-2i\left(\frac{2\mathbf{m}\pi\rho_\varepsilon}{\hbar^2}\right)^{1/2}e^{i\delta^l}\langle\psi_{v'l'}|V^\Omega_{\varepsilon\ell}|\psi^l_d\rangle, \tag{14}$$

for AI,[3] where[3,18,19] $V^\Omega_{\varepsilon\ell}(r)$ are given as

$$V^\Omega_{\varepsilon\ell}(r)\approx\alpha_\ell\left[\frac{\Gamma_\Omega(r)}{2\pi}\right]^{1/2}, \tag{15}$$

with $\Sigma_\ell|\alpha_\ell|^2=1$. In our calculations we set α_ℓ according to Khan *et al.*[20]

$$\alpha_\ell=\begin{cases}(1+\ell_{\max})^{-1/2}, & \ell\leqslant\ell_{\max}\\ 0, & \ell>\ell_{\max}.\end{cases} \tag{16}$$

In accord with Eq. (15) knowledge of the Ω dependent ionization widths $\Gamma_\Omega(r)$ leads directly to the Ω dependent S matrix. According to Gregor and Siska[4] (GS) the ionization width can be parametrized as

TABLE I. Parameters for the *ab initio* ionization widths.

Ω	p_1 (kcal/mole)	α_Ω (Å^{-1})	ρ_Ω (Å)	α_Ω/α_0	ρ_Ω/ρ_0
0	0.1121	2.775	1.8564	1.000	1.000
1	0.09055	2.794	1.7853	1.007	0.962
2	0.02546	3.189	1.4939	1.149	0.805

$$\Gamma_{\mathrm{GS}}(r)=A\exp[-\alpha(r-\rho)], \tag{17}$$

with $A=1$ kcal/mole, $\alpha=1.471$ Å^{-1}, and $\rho=0.531$ Å. This exponential gives good results in differential and total ionization cross sections for an unselected beam of $Ne^*(3s,{}^3P_2)$ and $Ne^*(3s,{}^3P_0)$.[4,6] For a beam of only $Ne^*(3s,{}^3P_2)$ atoms, Verheijen and Beijerinck (VB) have used the following parameters:[5] $A=1$ kcal/mole, $\alpha=1.848$ Å^{-1}, and $\rho=1.241$ Å.

The empirically derived ionization widths can be compared to *ab initio* calculations, such as those of Op de Beek *et al.*,[16] which can be fitted to the form

$$\Gamma(r)=p_1\exp[-\alpha(r-5\alpha_0)]. \tag{18}$$

The relevant parameters of this form, for our system, are summarized in Table I.

The *ab initio* α and ρ values turn out to be bigger than the empirically derived ones, yielding cross sections that are smaller than the experimental ones. Therefore we have adopted α and ρ values that are much closer to those of VB or GS.[4] In order to fine tune these values we note that according to Bussert and Op de Beek *et al.*[16] the ratio of the ionization rates for the ${}^3P_2$ Ω components is

$$\Gamma_B(\Omega=0):\Gamma_B(\Omega=1):\Gamma_B(\Omega=2)=1:0.75:0.016. \tag{19}$$

Table I shows that the $\Omega=0,1$ states have similar α_Ω and ρ_Ω parameters. Since according to Eq. (19) $\Gamma_B(\Omega=2)$ is considerably smaller than $\Gamma_B(\Omega=0,1)$, we can use the VB parameters α and ρ to model the $\Gamma(\Omega=0)$ ionization width. Using the VB values and the $\alpha_{1,2}/\alpha_0$ and $\rho_{1,2}/\rho_0$ ratios of Table I, we define "*ab initio* scaled" VB (VBS) ionization width parameters $\alpha_{1,2}$ and $\rho_{1,2}$ of $\alpha_0=1.848$ Å^{-1} and $\rho_0=1.241$ Å $\alpha_1=1.861$ Å^{-1} and $\rho_1=1.194$ Å and $\alpha_2=2.1233$ Å^{-1} and $\rho_2=0.999$ Å. In our calculations these values are used in Eq. (17) to define the imaginary part of the Ω dependent optical potentials.

Below we obtain the total ionization cross section as a function of the collision energy using the VBS ionization widths. In order to compare these values with the experimental ionization cross sections of Verheijen and Beijerinck,[5] we need to average the Ω dependent total ionization cross sections, $\sigma^{\mathrm{I}}_\Omega=\sigma^{\mathrm{PI}}_\Omega+\sigma^{\mathrm{AI}}_\Omega$. This is done using

$$\sigma^{\mathrm{I}}=(2J+1)^{-1}\sum_\Omega w_\Omega\sigma^{\mathrm{I}}_\Omega, \tag{20}$$

where the weight factor $w_\Omega=1$ for $\Omega=0$ and $w_\Omega=2$ for $\Omega=1,2$.

As can be seen in Fig. 1, the VBS Γ_Ω values reproduce quite well the qualitative behavior of σ^{I} (dashed line). However, the calculated values of σ^{I} are too small by a factor of 3/2 as compared to the experimental σ^{I} (dotted line). By

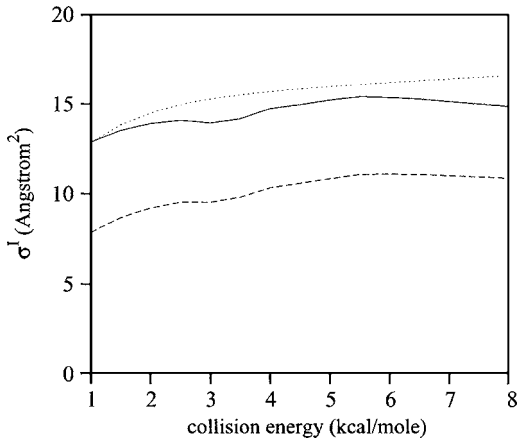

FIG. 1. The total ionization cross section σ^{I} as a function of the collision energy. The "*ab initio* scaled" or VBS ionization widths (dashed line), the ionization width obtained from scaling the α_Ω in the VBS by a factor 10/11 (solid line), and the experimental results of Verheijen and Beijerinck (Ref. 5) (dotted line).

comparison, Op de Beek *et al.*[16] used their *ab initio* Γ_Ω to calculate the total ionization cross section, with results smaller by a factor of 2 than the experimental values.

It is interesting to note that arbitrary rescaling of the α_Ω values in the VBS Γ_Ω, by a factor of 10/11, gives better agreement with experiment (solid line in Fig. 1). However, such scaling had little qualitative effect on the control studied below. Hence, for consistency, we use only the VBS parameters for the control calculations below.

D. Coherent control

Having obtained the Ω-dependent S matrices, the scattering amplitudes are obtained from Eq. (10), from which the fully differential cross sections for PI in the RAA are obtained as

$$\sigma_q(\hat{\mathbf{k}}_f,\varepsilon,\hat{\mathbf{k}}_\varepsilon;k,\mathbf{a}_\Omega)=\left|\sum_\Omega a_\Omega f_{q\Omega}(\hat{\mathbf{k}}_f,\varepsilon,\hat{\mathbf{k}}_\varepsilon;k)\right|^2, \tag{21}$$

where q indicates the exit channel. There are three possible exit channels characterized by the electronic state of the products $X\ ^2\Sigma^+_{1/2}$, $A_1\ ^2\Pi_{3/2}$, and $A_2\ ^2\Sigma_{1/2}$. The potential curves for the entrance and exit channels can be seen in Fig. 2. We link the entrance optical potential with each of the exit channels using Morgner's Γ splitting.[9,10]

The sum in Eq. (21) can be expanded to get

$$\sigma_q(\hat{\mathbf{k}}_f,\varepsilon,\hat{\mathbf{k}}_\varepsilon;k,\mathbf{a}_\Omega)=\sum_{\Omega\Omega'} a^*_{\Omega'}a_\Omega\sigma_{q\Omega'\Omega}, \tag{22}$$

with $\sigma_{q\Omega'\Omega}=f^*_{q\Omega'}f_{q\Omega}$. Since we are interested in the total ionization cross section we have to sum over all the exit channels and integrate over the solid angles $\hat{\mathbf{k}}_\varepsilon$ and $\hat{\mathbf{k}}_f$ and also over the emitted electron energy ε. It is easy to see from the form of the scattering amplitude that the integration over the solid angles yields a Kronecker delta function, thus simplifying the expressions for the $f^*_{q\Omega'}f_{q\Omega}$ products,

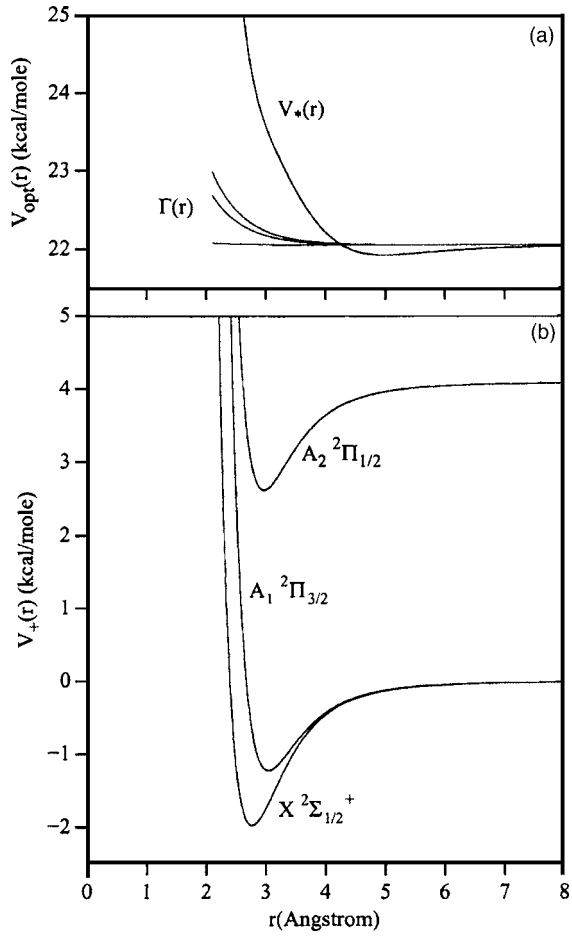

FIG. 2. Potential energy curves for $\Omega=0$. (a) The optical potential, $V_{\mathrm{opt}}(r)=V_*(r)-\frac{1}{2}i\Gamma(r)$, for the entrance channel. Also shown is the decomposition of Γ in the three exit channels. (b) The ion-atom potentials, $V_+(r)$, for the three exit channels.

$$f^*_{q\Omega'}f_{q\Omega}=\frac{\pi}{k^2}\sum_{\ell ll'}(2l+1)(2l'+1)\times\begin{pmatrix} l' & \ell & l\\ 0 & 0 & 0\end{pmatrix}^2 S^{l\Omega'*}_{l'\ell}(q,\varepsilon)S^{l\Omega}_{l'\ell}(q,\varepsilon), \tag{23}$$

where we have used the identity

$$\sum_{\mu=-\ell}^{\ell}\begin{pmatrix} l' & \ell & \bar{l}\\ -\mu & \mu & 0\end{pmatrix}\begin{pmatrix} l' & \ell & 1\\ -\mu & \mu & 0\end{pmatrix}=\frac{\delta_{l\bar{l}}}{2l+1}. \tag{24}$$

For s waves only we have that $\ell=0$, resulting in a simpler expression

$$f^*_{q\Omega'}f_{q\Omega}=\frac{\pi}{k^2}\sum_l(2l+1)^2S^{l\Omega'*}_{l0}(q,\varepsilon)S^{l\Omega}_{l0}(q,\varepsilon). \tag{25}$$

1. Preparation coefficients

After integrating over the energy of the emitted electron and summing over all exit channels, the dependence of the (PI or AI) cross sections on the vector of preparation coefficients $\mathbf{a}$ can be written schematically as

$$\sigma(\mathbf{a})=\sum_{\Omega'\Omega}a^*_{\Omega'}a_\Omega\sigma_{\Omega'\Omega}. \tag{26}$$

As a first try at coherently controlling PI and AI we use a superposition of only two $\Omega(=0,2)$ states because it can be rather easily created experimentally.[18] The cross section for this superposition state is

$$\sigma^{\mathrm{PI}}(\mathbf{a}) = |a_0|^2\sigma_0^{\mathrm{PI}} + |a_2|^2\sigma_2^{\mathrm{PI}} + 2\Re(a_0^* a_2 \sigma_{02}^{\mathrm{PI}}), \tag{27}$$

where $\sigma_{\Omega}^{\mathrm{PI}} = \sigma_{\Omega\Omega}^{\mathrm{PI}}$. Similar expressions for the associative ionization are obtained by summing over the exit channels and bound states,

$$\sigma^{\mathrm{AI}}(\mathbf{a}) = |a_0|^2\sigma_0^{\mathrm{AI}} + |a_2|^2\sigma_2^{\mathrm{AI}} + 2\Re(a_0^* a_2 \sigma_{02}^{\mathrm{AI}}). \tag{28}$$

As shown below, these formulas can be extended to the case of a linear superposition of $\Omega=0,1$ states.

The formulas developed here apply to both PI and AI. We therefore suppress the PI and AI indices, unless absolutely necessary. The preparation coefficients for both processes can be written in terms of Hopf coordinates in $\mathbb{C}^2$ as

$$a_0 = \sin\ \eta e^{i\xi_0}, \quad a_2 = \cos\ \eta e^{i\xi_2}, \tag{29}$$

where $\eta \in [0,\pi/2]$ and $\xi_{0,2} \in [0,2\pi]$. Using these coordinates Eq. (27) can be rewritten as

$$\sigma(\mathbf{a}) = \sigma_0 \sin^2\ \eta + \sigma_2 \cos^2\ \eta + 2|\sigma_{02}|\sin\ \eta \cos\ \eta \cos(\Delta\xi + \beta) \tag{30}$$

or

$$\sigma(\mathbf{a}) = \tfrac{1}{2}(\sigma_0+\sigma_2) - \tfrac{1}{2}(\sigma_0-\sigma_2)\cos 2\eta + |\sigma_{02}|\sin 2\eta \cos(\Delta\xi+\beta), \tag{31}$$

with $\Delta\xi = \xi_2 - \xi_0$ and $\beta = \arg\ \sigma_{0,2}$. It follows from Eq. (30) that for a fixed matrix $\sigma_{\Omega'\Omega}$ of Penning (associative) ionization cross sections, σ becomes a sole function of the preparation coefficients (initial state). We therefore plot the extent of control over PI or AI as a function of η and $\Delta\xi$.

The maxima and minima of $\sigma(\eta,\Delta\xi)$ are readily found by analyzing the solutions of the system of equations

$$\frac{\partial\sigma}{\partial\eta} = 2\sin\ \eta\cos\ \eta(\sigma_0-\sigma_2) + 2|\sigma_{02}|(\cos^2\ \eta - \sin^2\ \eta)\cos(\Delta\xi+\beta) = 0, \tag{32a}$$

$$\frac{\partial\sigma}{\partial\Delta\xi} = -2|\sigma_{02}|\sin\ \eta\cos\ \eta\sin(\Delta\xi+\beta) = 0. \tag{32b}$$

The second equation has as solutions

$$\Delta\xi = -\beta, \pi-\beta \quad \text{for any value of } \eta, \tag{33a}$$

$$\eta = 0, \pi/2 \quad \text{for any value of } \Delta\xi. \tag{33b}$$

Using the first of these solutions into Eq. (32a) gives after some trigonometry work

$$\eta_{\pm} = \frac{1}{2}\arctan\frac{\mp|\sigma_{02}|}{\sigma_0-\sigma_2}, \tag{34}$$

with η_+ and η_- the solutions for $\Delta\xi=-\beta$ and $\Delta\xi=\pi-\beta$, respectively. For our system $\sigma_0 > \sigma_2$, so a correct choice for the arctan (x) branches is

$$\eta_+ = \frac{\pi}{2} + \frac{1}{2}\arctan\frac{-|\sigma_{02}|}{\sigma_0-\sigma_2}, \tag{35a}$$

$$\eta_- = \frac{1}{2}\arctan\frac{|\sigma_{02}|}{\sigma_0-\sigma_2}. \tag{35b}$$

These solutions are symmetric with respect to $\eta=\pi/4$ and $\eta_+ + \eta_- = \pi/2$.

Replacing these solutions into Eq. (30) we obtain the maximal $(+)$ and minimal $(-)$ possible cross sections,

$$\sigma_{\pm} = \tfrac{1}{2}(\sigma_0+\sigma_2) \pm \tfrac{1}{2}\sqrt{(\sigma_0-\sigma_2)^2 + 4|\sigma_{02}|^2}. \tag{36}$$

A quantity of interest is the ratio between the associative ionization cross section and the total ionization cross section $\sigma^{\mathrm{I}} = \sigma^{\mathrm{PI}} + \sigma^{\mathrm{AI}}$,

$$C(\eta,\Delta\xi) = \frac{\sigma^{\mathrm{AI}}}{\sigma^{\mathrm{I}}}. \tag{37}$$

III. RESULTS

Figures 3 and 4 display the Penning and associative ionization cross sections, as well as the ratio $\sigma^{\mathrm{AI}}/\sigma^{\mathrm{I}}$, as functions of the preparation coefficients for initial states comprising $\Omega=0,2$ and $\Omega=0,1$. These results are obtained for collision energy $E=2.0$ kcal/mole using the VBS ionization widths. Results show a wide range of controlled values for the Penning ionization and associative ionization cross sections. Indeed, graphical limitations prevent presenting the entire contour range. Hence, for example, in Fig. 4, panel (a) the minimum Penning ionization cross section is as small as 2×10^{-2}, in panel (b) the minimum is 10^{-4}, and the ratio in panel (c) varies from 0.025 to 0.85. These maxima and minima are best seen in Figs. 5 and 6. Note that at some values of the control parameters, both the Penning and associative ionization cross sections are on the order of 0.05 Å^2, so that the total reaction cross section is very small.

In Figs. 5 and 6 we have plotted the maxima and minima of the different σ for all energies considered between 1 and 8 kcal/mole. We note that the locations of the maxima and minima are only weakly dependent on the collision energy. In general σ^{PI} increases monotonically with the energy, while σ^{AI} displays a maximum at about $E=2.0$ kcal/mole. A direct comparison of Figs. 5 and 6 demonstrates better control for the $\Omega=0,1$ linear combination. All cross sections were computed using the values of α of Table I.

Inspection of Figs. 3 and 4 shows that PI and AI can be effectively switched off by judiciously choosing the preparation coefficients of the initial superposition state in the $\Omega=0,1$ case. This is also true for AI (but not for PI) in the $\Omega=0,2$ superposition case.

The fact that the dashed line in Fig. 1 shows good qualitative agreement with the experimental values indicates that our cross sections are qualitatively correct as functions of collisional energy, although they are smaller than the experimental ones. Thus far, there are no experimental values for the cross section for M selected $\mathrm{Ne}^*(3s,{}^3P_2)$ states. The availability of such results would allow a better assessment

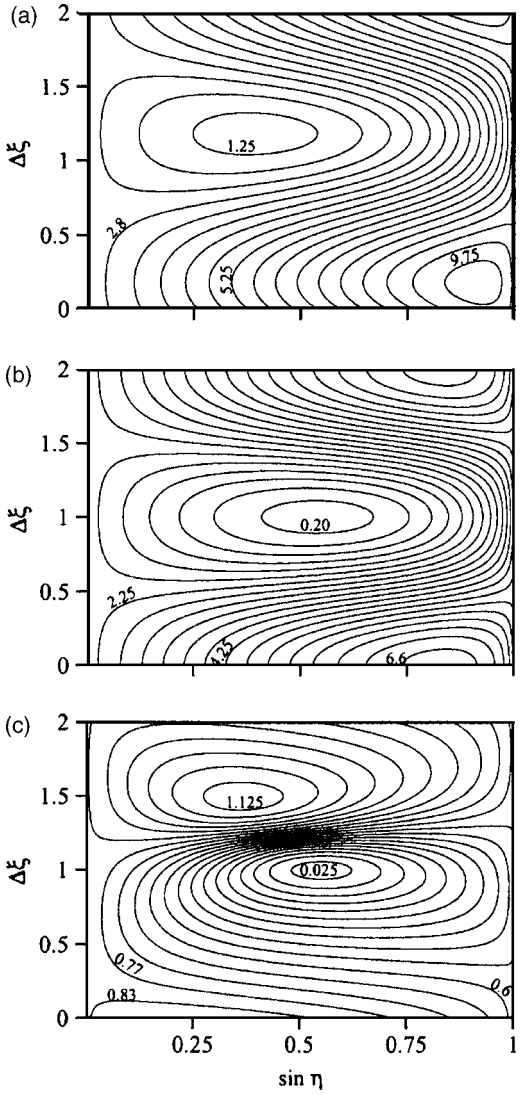

FIG. 3. Contours of constant σ as a function of the control parameters $(\sin\eta, \Delta\xi)$ for an initial superposition of $\Omega=0,2$ states. The results were obtained using the VBS Γ_Ω whose real part is that of GS. The collision energy is $E=2$ kcal/mole. (a) σ^{PI}, (b) σ^{AI}, and (c) σ^{AI}/σ^{PI}.

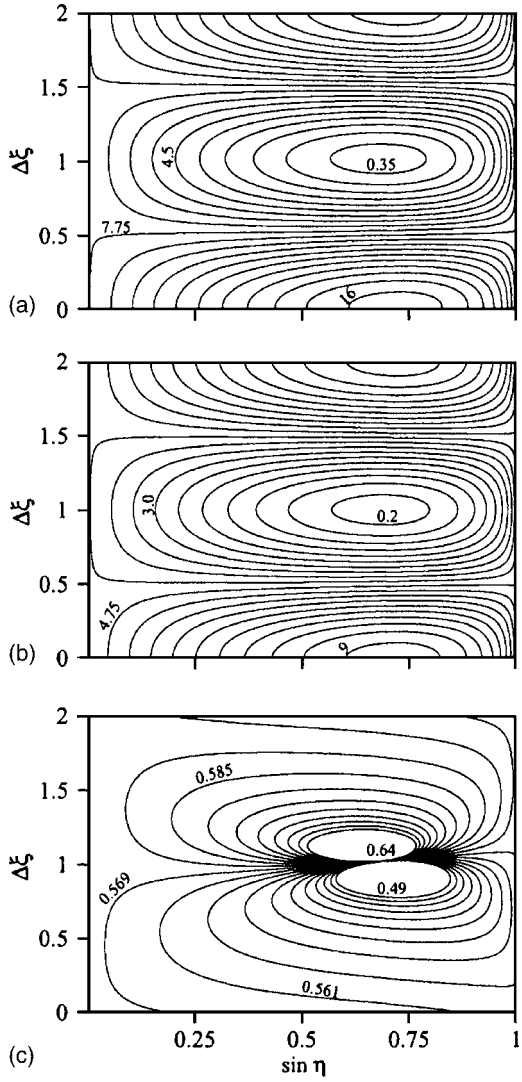

FIG. 4. As in Fig. 3, but for a superposition of $\Omega=0,1$ states. (a) σ^{PI}, (b) σ^{AI}, and (c) σ^{AI}/σ^{PI}.

of the quality of the computed results. We look forward to such results emerging from modern experimental efforts.

IV. CONCLUSIONS

We have shown that it is possible to control the Penning and associative ionization cross sections in the $Ar+Ne^*(\Omega)$ collision. The control is based on preparing a superposition of either the $\Omega=0,2$ or $\Omega=0,1$ angular momentum states. Our demonstration is based on numerical calculations which make use of empirically derived, *ab initio* scaled, VB optical potentials (VBS).

An interesting outcome of our calculations is the possibility of essentially switching off PI and AI cross sections. This suggests the presence of strong quantum effects that could be observed in scattering experiments.

A potential application of the methods developed in this paper is the study of the suppression of PI or AI in cold collisions in crossed beam experiments. As the collisional energy is lowered the colliding atoms approach each other more slowly, making the PI or AI cross section larger. Coherent control on the cross section could show dramatic effects of suppression of PI or AI. Studies of this kind are under way.

ACKNOWLEDGMENTS

We thank Professor Peter Siska for his generosity in providing us with his computer programs and Professor Klaas Bergmann for extensive discussions. This work was supported by the Natural Sciences and Engineering Research Council of Canada.

APPENDIX: SCATTERING AMPLITUDE

The basic formulas used here follow the works of Hickman and Morgner,[18] Morgner,[19] and Bieniek[21] who obtained expressions for the center of mass scattering amplitudes for PI and AI based on O'Malley's theory of dissociative attachment.[22,23] Earlier theoretical treatments of PI and AI can be found in the works of Mori and Fujita,[24] Mori,[25,26] Nakamura,[27,28] and Miller[29] among others.

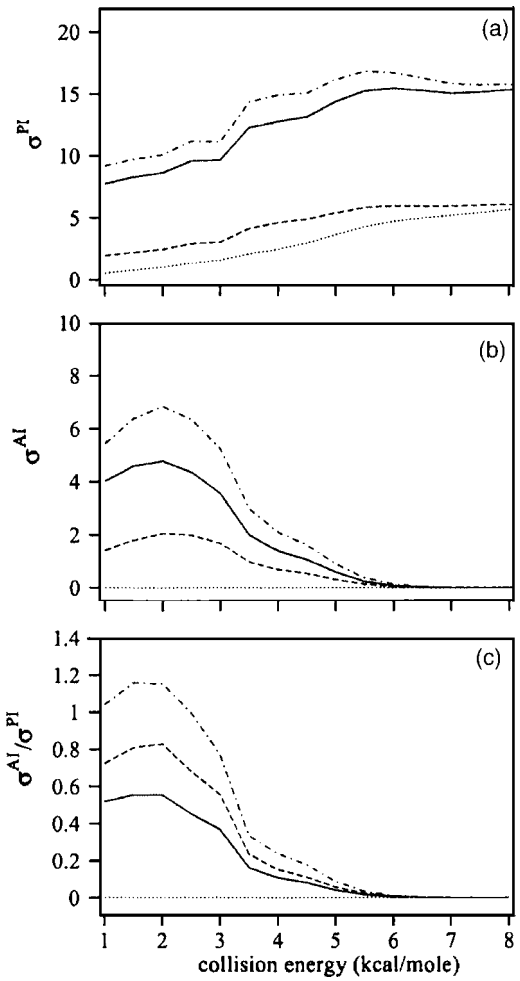

FIG. 5. Maxima and minima of control over the cross section for an initial superposition of $\Omega=0,2$ states. (a) σ^{PI}, (b) σ^{AI}, and (c) σ^{AI}/σ^{PI}. $\Omega=0$, solid line; $\Omega=2$, dashed line; the maxima σ_{max} are shown as dot-dashed curves; and the minima σ_{min} are shown as dotted curves.

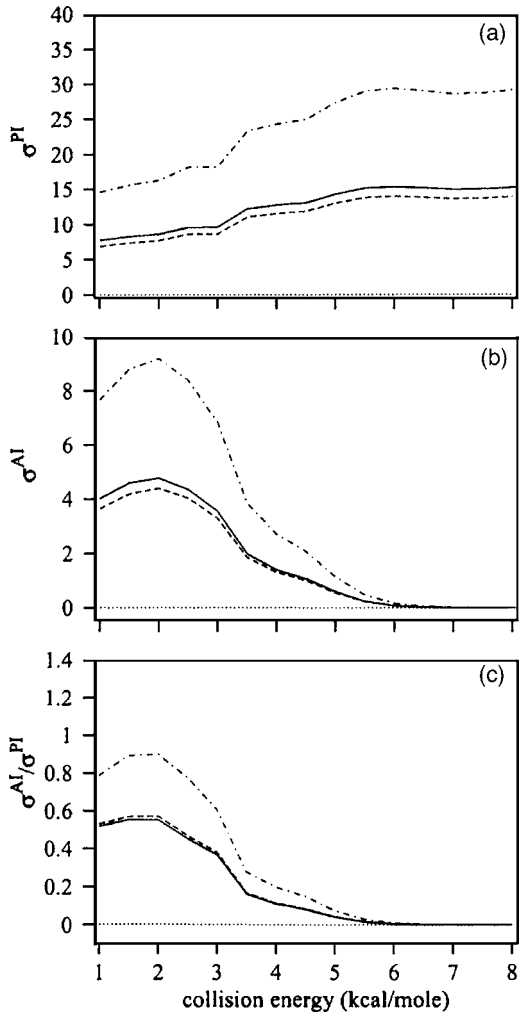

FIG. 6. As in Fig. 5, but for an initial superposition of $\Omega=0,1$ states.

Prior to the collision the asymptotic internuclear momentum vector is $\mathbf{k}=\{k,\hat{\mathbf{k}}\}$. After the collision the internuclear momentum vector is denoted as $\mathbf{k}_f=\{k_f,\hat{\mathbf{k}}_f\}$. The momentum direction of the departing Penning electron is denoted as $\hat{\mathbf{k}}_\varepsilon$ and its energy as ε. The interatomic separation vector is denoted as $\mathbf{r}=\{r,\hat{\mathbf{r}}\}$.

The energy of the emitted electron is related to the collisional energy E and the energy of the nuclei after the collision E' by the conservation of energy

$$E+\varepsilon_0=\varepsilon+E', \tag{A1}$$

with $\varepsilon_0=E_*-\mathrm{IE}$, the difference between the excitation energy of the metastable atom (Ne^*) and the ionization energy of the target atom (Ar).

The scattering amplitude, which is exact within the Born-Oppenheimer approximation, is given by[18,19,30]

$$f(\hat{\mathbf{k}}_f,\varepsilon,\hat{\mathbf{k}}_\varepsilon;\mathbf{k})=-\frac{2\mathbf{m}\rho_\varepsilon^{1/2}}{(4\pi\hbar)^2}\left(\frac{k_f}{k}\right)^{1/2}\langle\psi_\varepsilon|V_{\varepsilon,\hat{\mathbf{k}}_\varepsilon}|\psi_d\rangle, \tag{A2}$$

where $\mathbf{m}$ is the reduced mass of the nuclei and ρ_ε is the density of the electronic continuum states. $\psi_d(\mathbf{r})$ is the incoming wave function scattered by the optical potential $V_*(r)-(i/2)\Gamma(r)$, which has partial wave expansion

$$\psi_d(\mathbf{r})=4\pi\sum_{l=0}^{\infty}\sum_{m=-l}^{+l} i^l e^{l\delta^l}\frac{\psi_d^l(r)}{k^{1/2}r}Y_{lm}^*(\hat{\mathbf{k}})Y_{lm}(\hat{\mathbf{r}}), \tag{A3}$$

where

$$\psi_d^l(r)\xrightarrow{r\to\infty}k^{-1/2}\sin(kr-\pi l/2+\delta^l),$$

with δ^l being complex phase shifts that account for the loss of flux due to ionization. The function $\psi_\varepsilon(\mathbf{r})$ describes the system on the exit potential $V_+(r)$, its partial wave expansion being

$$\psi_\varepsilon(\mathbf{r})=4\pi\sum_{l'=0}^{\infty}\sum_{m'=-l'}^{+l'} i^{l'}e^{-i\delta_f^{l'}}\frac{\psi_\varepsilon^{l'}(r)}{k_f^{1/2}r}Y_{l'm'}^*(\hat{\mathbf{k}}_f)Y_{l'm'}(\hat{\mathbf{r}}),$$

$$\psi_\varepsilon^{l'}(r)\xrightarrow{r\to\infty}k_f^{-1/2}\sin(k_fr-\pi l'/2+\delta_f^{l'}), \tag{A4}$$

with $\delta_f^{l'}$ being real phase shifts.

The electronic part of the scattering amplitude of Eq. (A2) is incorporated in $V_{\varepsilon,\hat{\mathbf{k}}_\varepsilon}(\mathbf{r})$, the probability amplitude for the emission of an electron with ε, and $\hat{\mathbf{k}}_\varepsilon$ for frozen nuclei. Before the collision there are N bound electrons, whose po-

sitions relative to the molecular-fixed frame are given by $\mathbf{R}'_N$. After ionization there are $N-1$ bound electrons, described in the molecular-fixed frame by $\mathbf{R}'_{N-1}$, and one "free" electron, described in the center of mass frame by the $\mathbf{R}=\{R,\hat{\mathbf{R}}\}$ position vector.

Given the above definition we can write $V_{\varepsilon,\hat{\mathbf{k}}_\varepsilon}(\mathbf{r})$ as

$$V_{\varepsilon,\hat{\mathbf{k}}_\varepsilon}(\mathbf{r})=\langle\phi_{\varepsilon,\hat{\mathbf{k}}_\varepsilon}|H|\phi_N\rangle_{\mathbf{R}}, \tag{A5}$$

where the $\langle\phi|H|\phi'\rangle_{\mathbf{R}}$ implies integration with respect to the electronic coordinates. The operator H is obtained using Feshbach projection operators formalism.[30]

The initial metastable electronic wave function is $\phi_N(\mathbf{R}'_N;r)$ and the final electronic wave function is $\phi_{\varepsilon,\hat{\mathbf{k}}_\varepsilon}(\mathbf{R},\mathbf{R}'_{N-1};r)$. According to Miller *et al.*[30] the final electronic wave function can be factorized as

$$\phi_{\varepsilon,\hat{\mathbf{k}}_\varepsilon}(\mathbf{R},\mathbf{R}'_{N-1};r)=\chi_{\varepsilon,\hat{\mathbf{k}}_\varepsilon}(\mathbf{R})\phi_{N-1}(\mathbf{R}'_{N-1};r). \tag{A6}$$

The wave function of the emitted electron can also be expanded in partial wave as

$$\chi_{\varepsilon,\hat{\mathbf{k}}_\varepsilon}(\mathbf{R})=4\pi\sum_{\ell=0}^{\infty}\sum_{\mu=-\ell}^{+\ell} i^\ell e^{i\sigma^\ell}\frac{\chi^\ell_\varepsilon(R)}{R}Y^*_{\ell\mu}(\hat{\mathbf{k}}_\varepsilon)Y_{\ell\mu}(\hat{\mathbf{R}}). \tag{A7}$$

When into Eq. (A5) the above expansion yields

$$V_{\varepsilon,\hat{\mathbf{k}}_\varepsilon}(\mathbf{r})=4\pi\sum_{\ell=0}^{\infty}\sum_{\mu=-\ell}^{+\ell}\left(\frac{4\pi}{2\ell+1}\right)^{1/2}V_{\varepsilon\ell}(r)Y_{\ell\mu}(\hat{\mathbf{k}}_\varepsilon)Y^*_{\ell\mu}(\hat{\mathbf{r}}), \tag{A8}$$

where

$$V_{\varepsilon\ell}(r)=i^{-\ell}e^{-i\sigma^\ell}\langle\chi^\ell_\varepsilon Y_{\ell0}\phi_{N-1}|H|\phi_N\rangle_{\mathbf{R}}. \tag{A9}$$

Using the above expression, the scattering amplitude $f=f(\hat{\mathbf{k}}_f,\varepsilon,\hat{\mathbf{k}}_\varepsilon;\mathbf{k})$, of Eq. (A2), can be written as

$$\begin{aligned}f=&-\frac{16\mathbf{m}\rho_\varepsilon^{1/2}\pi^{3/2}}{\hbar^2k}\sum_{\ell,\mu,l,m,l',m'} i^{l-l'}e^{i(\delta^l+\delta^{l'}_f)}\\&\times(2\ell+1)^{-1/2}Y_{l'm'}(\hat{\mathbf{k}}_f)Y^*_{lm}(\hat{\mathbf{k}})Y_{\ell\mu}(\hat{\mathbf{k}}_\varepsilon)\\&\times\langle\psi^{l'}_\varepsilon Y_{l'm'}|V_{\varepsilon\ell}Y^*_{\ell\mu}|\psi^l_dY_{lm}\rangle,\end{aligned} \tag{A10}$$

where the sums over ℓ, μ, l, m, l', and m' are the same as in Eqs. (A7), (A3), and (A4). The integral can be factorized in a radial and angular part, giving

$$\langle\psi^{l'}_\varepsilon Y_{l'm'}|V_{\varepsilon\ell}Y^*_{\ell\mu}|\psi^l_dY_{lm}\rangle=\langle Y_{l'm'}|Y^*_{\ell\mu}|Y_{lm}\rangle\langle\psi^{l'}_\varepsilon|V_{\varepsilon\ell}|\psi^l_d\rangle, \tag{A11}$$

and the angular part expressed in terms of Wigner 3-j symbols,[31]

$$\begin{aligned}&\langle Y_{l'm'}|Y^*_{\ell\mu}|Y_{lm}\rangle\\&=(-1)^m\left[\frac{(2l'+1)(2\ell+1)(2l+1)}{4\pi}\right]^{1/2}\\&\times\begin{pmatrix}l'&\ell&l\\0&0&0\end{pmatrix}\begin{pmatrix}l'&\ell&l\\m'&\mu&-m\end{pmatrix}.\end{aligned} \tag{A12}$$

The coefficients of the 3-j symbols in Eq. (A12) give the rules for the conservation of the orbital angular momentum and its z-axis projection,

$$l'=|l-\ell|,\ldots,l+\ell,\quad m'=m-\mu. \tag{A13}$$

For the radial part, we introduce the partial wave S matrix

$$S^l_{l'\ell}(\varepsilon)=-i\frac{4\mathbf{m}\rho_\varepsilon^{1/2}}{\hbar^2}e^{i(\delta^l+\delta^{l'}_f)}\langle\psi^{l'}_\varepsilon|V_{\varepsilon\ell}|\psi^l_d\rangle. \tag{A14}$$

The scattering amplitude now reads

$$\begin{aligned}f=&\frac{2\pi}{ik}\sum_{\ell,\mu,l,m,l'} i^{l-l'}(-1)^m[(2l+1)(2l'+1)]^{1/2}\begin{pmatrix}l'&\ell&l\\0&0&0\end{pmatrix}\\&\times\begin{pmatrix}l'&\ell&l\\m'&\mu&-m\end{pmatrix}\times S^l_{l'\ell}(\varepsilon)Y_{l'm'}(\hat{\mathbf{k}}_f)Y^*_{lm}(\hat{\mathbf{k}})Y_{\ell\mu}(\hat{\mathbf{k}}_\varepsilon).\end{aligned} \tag{A15}$$

When the space-fixed z axis is chosen to lie along $\mathbf{k}$ we have $\hat{\mathbf{k}}=(0,0)$, and the scattering amplitude is given as

$$\begin{aligned}f=&\frac{\pi^{1/2}}{ik}\sum_{\ell,\mu,l,l'} i^{l-l'}(2l+1)(2l'+1)^{1/2}\begin{pmatrix}l'&\ell&l\\0&0&0\end{pmatrix}\\&\times\begin{pmatrix}l'&\ell&l\\-\mu&\mu&0\end{pmatrix}S^l_{l'\ell}(\varepsilon)Y_{l'-\mu}(\hat{\mathbf{k}}_f)Y_{\ell\mu}(\hat{\mathbf{k}}_\varepsilon).\end{aligned} \tag{A16}$$

[1] M. Shapiro and P. Brumer, *Principles of the Quantum Control of Molecular Processes* (Wiley, Hoboken, NJ, 2003).
[2] P. Brumer, A. Abrashkevich, and M. Shapiro, Faraday Discuss. **113**, 291 (1999).
[3] P. E. Siska, Rev. Mod. Phys. **65**, 337 (1993).
[4] R. W. Gregor and P. E. Siska, J. Chem. Phys. **74**, 1078 (1981).
[5] M. J. Verheijen and H. C. W. Beijerinck, Chem. Phys. **102**, 255 (1986).
[6] E. R. T. Kerstel, M. F. M. Janßens, K. A. H. van Leeuwen, and H. C. W. Beijerinck, Chem. Phys. **119**, 325 (1988).
[7] J. Baudon, P. Feron, C. Miniatura, F. Perales, J. Reinhardt, J. Robert, H. Haberland, B. Brunetti, and F. Vecchiocattivi, J. Chem. Phys. **95**, 1801 (1991).
[8] D. Hausamann and H. Morgner, Mol. Phys. **54**, 1085 (1985).
[9] H. Morgner, Comments At. Mol. Phys. **11**, 271 (1982).
[10] H. Morgner, J. Phys. B **18**, 251 (1985).
[11] H. Hotop, J. Lorenzen, and A. Zastrow, J. Phys. B **18**, 251 (1985).
[12] W. Bußert, T. Bregel, J. Ganz, K. Harth, A. Siegel, M. W. Ruf, and H. Hotop, J. Phys. (Paris), Colloq. **46**, C1 (1985).
[13] W. Bußert, T. Bregel, R. J. Allan, M. W. Ruf, and H. Hotop, Z. Phys. A Atoms and Nuclei **320**, 105 (1985).
[14] T. Bregel, W. Bußert, J. Ganz, H. Hotop, and M. W. Ruf, in *Electronic and Atomic Collisions*, edited by D. C. Lorents, W. E. Meyerhof, and J. R. Peterson (North-Holland, Amsterdam, 1986), pp. 577–584.
[15] J. P. J. Drießen, S. S. O. de Beek, L. M. T. Somers, H. C. W. Biejerinck, and B. J. Varhaar, Phys. Rev. A **44**, 167 (1991).
[16] S. S. Op de Beek, J. P. J. Drießen, S. J. J. M. F. Kokkelmans, W. Boom, H. C. W. Biejerinck, and B. J. Varhaar, Phys. Rev. A **56**, 2792 (1997).
[17] M. Mori, T. Watanabe, and K. Katsuura, J. Phys. Soc. Jpn. **19**, 380 (1964).
[18] F. Vewinger, M. Heinz, R. G. Fernandez, N. V. Vitanov, and K. Bergmann, Phys. Rev. Lett. **91**, 213001 (2003); M. Heinz, F. Vewinger, U. Schneider, L. P. Yatsenko, and K. Bergmann, Opt. Commun. **264**, 248 (2006); M. V. Vitanov, M. Fleischauer, B. W. Shore, and K. Bergmann, Adv. At., Mol., Opt. Phys. **46**, 55 (2001).
[19] A. P. Hickman and H. Morgner, J. Phys. B **9**, 1765 (1976); H. Morgner, J. Phys. B **11**, 269 (1978).
[20] A. Khan, H. R. Siddiqui, and P. E. Siska, J. Chem. Phys. **95**, 3371 (1991).
[21] R. J. Bieniek, Phys. Rev. A **18**, 392 (1978).

[22] T. F. O'Malley, Phys. Rev. **150**, 14 (1966).
[23] T. F. O'Malley, Phys. Rev. **156**, 230 (1967).
[24] M. Mori and H. Fujita, J. Phys. Soc. Jpn. **20**, 432 (1965).
[25] M. Mori, J. Phys. Soc. Jpn. **21**, 979 (1966).
[26] M. Mori, J. Phys. Soc. Jpn. **26**, 773 (1969).
[27] H. Nakamura, J. Phys. Soc. Jpn. **26**, 1473 (1969).
[28] H. Nakamura, J. Phys. Soc. Jpn. **31**, 574 (1971).
[29] W. H. Miller, J. Chem. Phys. **52**, 3563 (1970).
[30] W. H. Miller, C. A. Slocomb, and H. F. Schaefer III, J. Chem. Phys. **56**, 1347 (1972).
[31] M. E. Rose, *Elementary Theory of Angular Momentum* (Dover, New York, 1957).